



26 **Abstract**

27 Rapid evolution of SARS-CoV-2 has resulted in the emergence of numerous variants, posing  
28 significant challenges to public health surveillance. Clinical genome sequencing, while valuable,  
29 has limitations in capturing the full epidemiological dynamics of circulating variants in the  
30 general population. This study utilized receptor-binding domain (RBD) amplicon sequencing of  
31 wastewater samples to monitor the SARS-CoV-2 community dynamics and evolution in El Paso,  
32 TX. Over 17 months, we identified 91 variants and observed waves of dominant variants  
33 transitioning from BA.2 to BA.2.12.1, BA.4&5, BQ.1, and XBB.1.5. Our findings demonstrated  
34 early detection of variants and identification of unreported outbreaks, while showing strong  
35 consistency with clinical genome sequencing data at the local, state, and national levels. Alpha  
36 diversity analyses revealed significant periodical variations, with the highest diversity observed  
37 in winter and the outbreak lag phases, likely due to lower competition among variants before the  
38 outbreak growth phase. The data underscores the importance of low transmission periods for  
39 rapid mutation and variant evolution. This study highlights the effectiveness of integrating RBD  
40 amplicon sequencing with wastewater surveillance in tracking viral evolution, understanding  
41 variant emergence, and enhancing public health preparedness.

42

43 **Keywords:** Receptor-binding domain, amplicon sequencing, Wastewater surveillance, SARS-  
44 CoV-2, variant emergence, viral evolution

45

46

47

48

49

50

51

52

53

54

## 55 Introduction

56 SARS-CoV-2, the virus responsible for COVID-19, has undergone significant evolution since its  
57 emergence, leading to waves of outbreaks by multiple variants such as Alpha, Beta, Gamma,  
58 Delta, and Omicrons. Each of these variants exhibits distinct characteristics in terms of  
59 transmissibility, pathogenicity, and ability to evade immune responses. A key driver of this  
60 evolution is the mutation of the spike-protein-encoding gene, particularly in the receptor-binding  
61 domain (RBD), which is crucial for the virus's ability to bind to host cell receptors and initiate  
62 infection<sup>1-3</sup>. Mutations in the RBD can enhance the virus's ability to spread and escape immune  
63 detection<sup>4</sup>, making it a critical focus for variant tracking and public health monitoring. For  
64 example, the Delta variant harbors the L452R and T478K mutations which increases binding  
65 affinity to ACE2 receptor on host cells and contributes to reduced vaccine efficacy<sup>5-9</sup>.  
66 Understanding and tracking these variants are crucial for managing ongoing and future  
67 outbreaks.

68 Traditional surveillance methods, such as genome sequencing of clinically ascertained samples,  
69 have been instrumental in identifying and tracking SARS-CoV-2 variants. However, these  
70 methods are often time-consuming, expensive, and resource-intensive<sup>10-12</sup>. Moreover, clinical  
71 testing primarily captures data from symptomatic individuals, potentially missing large portions  
72 of the infected population who are asymptomatic or pre-symptomatic<sup>13-16</sup>. In contrast,  
73 wastewater surveillance has emerged as a promising approach to monitor community-level  
74 prevalence and diversity of SARS-CoV-2. By analyzing wastewater samples, one can detect  
75 viral RNA shed by infected individuals, regardless of their symptom status<sup>17-19</sup>. Wastewater  
76 surveillance offers several advantages, including non-invasiveness, cost-effectiveness, and the  
77 ability to capture data from a broad segment of the population. This method has now been  
78 widely implemented globally, providing early warnings of outbreaks and offering a  
79 comprehensive view of community-level viral transmission.

80 Wastewater sequencing is a crucial tool for early detection of viral variants. By collecting and  
81 analyzing the nucleic acids in wastewater using next-generation sequencing, researchers can  
82 identify mutations and new variants weeks before they appear in clinical samples<sup>20-22</sup>. This  
83 method allows continuous tracking of variant dynamics and provides a more complete picture of  
84 the viral landscape<sup>23-26</sup>. However, the complex nature of wastewater, containing a mixture of  
85 genetic material from various sources, complicates data analysis and interpretation, posing  
86 challenges in genome assembly, variant assignment/classification, and sequencing accuracy<sup>27-</sup>  
87 <sup>32</sup>. Typically, wastewater sequencing relies on tiled amplicon amplification to recover the whole

88 genome due to low concentrations. A simpler approach targets the spike genes, particularly the  
89 RBD, with specific target areas varying among studies<sup>21,33–38</sup>. While existing research has  
90 primarily focused on the detection and surveillance of variants, there has been limited  
91 exploration into the epidemiological dynamics and patterns of variant emergence and evolution  
92 within community wastewater.

93 In this study, we targeted the receptor-binding domain region and developed a streamlined  
94 bioinformatic pipeline to track the variant dynamics of SARS-CoV-2 over 17 months using  
95 wastewater samples from El Paso, a border city in west Texas, US, and Ciudad Juárez, Mexico.  
96 We compared our wastewater data with clinical genome sequencing results at local, state, and  
97 national levels to assess consistency and reliability. Additionally, we conducted epidemiological  
98 dynamic analyses to uncover patterns of variant evolution and emergence. By integrating RBD  
99 amplicon sequencing with wastewater surveillance, this research offers an innovative approach  
100 to understanding variant emergence and evolution, enriching the surveillance toolkit to  
101 anticipate and mitigate emerging threats in the post-pandemic era.

102

## 103 **2. Materials and Methods**

### 104 2.1 Wastewater sampling

105 Composite wastewater samples (24-hr) were collected weekly from March 14th, 2022, to August  
106 8th, 2023, from three wastewater treatment plants (WWTPs) in the City of El Paso, Texas. The  
107 WWTPs A, B, and C serve 98,754, 125,462, and 128,003 residents, respectively. The daily total  
108 wastewater flow volume was measured and provided by El Paso Water. Samples were shipped  
109 overnight in ice boxes to the laboratory and processed on the day of receipt. The rest of the raw  
110 samples were stored at -80 °C.

### 111 2.2 Wastewater sample processing, RNA extraction, and RT-qPCR

112 Samples were processed based on previous methods<sup>39–41</sup>. Briefly, 50 mL wastewater samples  
113 were first centrifuged at 3000 g for 10 min at 4°C. The supernatant was collected and further  
114 filtered with MilliporeSigma™ Steriflip™ Sterile Disposable Vacuum Filter Units. Then, the 15  
115 mL filtrates were concentrated to ~200uL with MilliporeSigma™ Amicon™ Ultra-15 Centrifugal  
116 Filter Units. The enriched samples were subject to RNA extraction with QIAamp Viral RNA Mini  
117 Kit according to the manufacturer's protocol. RNA was eluted with 100 uL nuclease-free water  
118 and stored at -20°C.

119 SARS-CoV-2 was tested and quantified using the US CDC N1 real-time PCR assay (Biorad,  
120 CFX96 C1000 Touch) using the following program: 50 °C 10 min for reverse transcription, 95 °C  
121 20 s for RT inactivation and initial denaturation, and 48 cycles of denature (95 °C, 1 s) and  
122 anneal/extend (60 °C, 30 s). At least two negative controls were included in every PCR run.  
123 Pepper mild mottle virus (PMMoV) was also measured as an internal reference for sample  
124 processing and variations in wastewater flow and/or fecal materials, as previously reported<sup>40,42</sup>.  
125 Two technical replicates were performed for all RT-qPCR reactions. SARS-CoV-2 RNA  
126 concentrations were adjusted by the corresponding PMMoV concentrations in the sample using  
127 the method described in previous work<sup>40,42</sup>. The total viral load per capita was calculated for  
128 data comparison across sewersheds with the following formula:

129 
$$\text{Viral load} = \text{RNA concentraion} \times \text{Dilution factor} \times \text{Flow rate}$$

130 
$$\text{Viral load per capita} = \frac{\text{Viral concentration}}{\text{Population covered by the WWTP}} * 100,000$$

131 The Dilution Factor is the scale of enrichment during the experiment, which is 6.7 (100 uL/15  
132 mL). This indicates that 15 mL of raw composite wastewater sample was concentrated into 100  
133 uL of RNA.

### 134 2.3 Preparation of synthetic SARS-CoV-2 variant communities

135 The SARS-CoV-2 Wuhan-Hu strain and Omicron BA.4&5 genomes were purchased from  
136 TWIST Bioscience. Original stocks were diluted one thousand-fold before mixing with four  
137 different ratios: 10%:90%, 25%:75%, 50%:50%, and 90%:10%. 10 ul of each mixture sample  
138 were then subjected to RNA extraction with QIAamp Viral RNA Mini Kit.

### 139 2.4 RBD amplicon amplification of wastewater samples

140 Primers for amplifying the receptor-binding domain (RBD) of the SARS-CoV-2 spike  
141 glycoprotein were provided in Table S1 and adapted from a previous study<sup>20</sup>. This amplicon  
142 amplifies 168 amino acids from 337 to 504 aa, covering almost the entire receptor-binding motif  
143 of SARS-CoV-2 (from 437 to 508 aa) and most receptor-binding domain (from 319 to 541 aa).  
144 Briefly, wastewater samples and positive control RNA were transcribed into cDNA using  
145 SuperScript™ IV Reverse Transcriptase (ThermoFisher Scientific, USA). The RBD amplicon  
146 was then amplified from the cDNA using primers S008 and S012 in a first PCR with Q5® High-  
147 Fidelity 2X Master Mix (New England Biolabs, USA), under the following conditions: polymerase  
148 activation at 95°C for 2 minutes, followed by 30 cycles of denaturation at 95°C for 1 second,

149 annealing at 72°C for 30 seconds, and extension at 60°C for 30 seconds. A second PCR was  
150 performed to add Illumina overhangs to the RBD amplicon using primers S009 and S013, with  
151 the same conditions but for 40 cycles. The PCR product was purified using AMPure XP beads  
152 and eluted with 30 µL of nuclease-free water. For testing the protocol, synthetic SARS-CoV-2  
153 Wuhan-Hu strain and Omicron BA.4&5 genomes from TWIST Bioscience were diluted 1,000-  
154 fold, and four mixtures were prepared in ratios of 10%:90%, 25%:75%, 50%:50%, and  
155 90%:10%. 10 µL of each mixture was used for RNA extraction, amplicon amplification, library  
156 preparation, and sequencing.

## 157 2.5 Library preparation and sequencing data analysis

158 The purified PCR amplicons were dual-indexed using NEBNext Multiplex Oligos (New England  
159 Biolabs, USA) for Illumina and further purified using AMPure XP beads. Libraries were pooled  
160 based on their concentrations and sequenced on a 300 paired-end Miseq run at the ATGC  
161 Facility at MD Anderson Cancer Center. The raw sequencing data in fastq format were de-  
162 multiplexed. DADA2 package (version 4.3.0)<sup>43</sup> was used to filter and trim sequences, merge  
163 paired ends, and remove chimeras in Rstudio version 4.3.2. The unique amplicon sequence  
164 variants (ASVs) were aligned and identified using the BLAST online tool<sup>44</sup> using the  
165 Betacoronavirus database. For each ASV, the top 10 BLAST results containing the Pango  
166 Lineage name with the highest alignment scores (ranging from 99% to 100%) were  
167 downloaded, and the most frequent variant was identified as the variant for that sequence. The  
168 relative abundance of each variant was calculated by the ratio of the count of each variant to the  
169 total sequence count. Variants with relative abundance higher than 10% on at least one sample  
170 were designated as major variants. The remaining variants were grouped as 'others' for plotting  
171 and visualization purposes.

## 172 2.6 COVID-19 cases and genome data

173 The reported COVID-19 case data by lab-testing diagnostics was downloaded from  
174 healthdata.gov, and the 7-day rolling average was used for further analysis and data  
175 visualization. The Texas-specific data was extracted according to the state name label. SARS-  
176 CoV-2 genome data for the study period was obtained from the GISAID EpiCoV™ database  
177 using the GISAIDR (version 0.9.9) package in R<sup>45</sup>. The variants were assigned by Pango v.4.3  
178 by GISAID. Only records with complete genomes were downloaded. The number of each  
179 variant per week was counted, and the relative abundance was calculated accordingly.

180

## 181 Results

### 182 3.1 RBD amplicon sequencing of wastewater reveals temporal dynamics of SARS-CoV-2 183 variants circulating in the city.

184 To validate the RBD amplicon sequencing approach for variant identification, we utilized  
185 synthetic mock variant communities. Four mock communities were prepared by mixing the  
186 original SARS-CoV-2 Wuhan-Hu strain (Wild Type) and the BA.4&5 strain at ratios of 10%:90%,  
187 25%:75, 50%:50%, and 90%:10%. Each mock community underwent RNA extraction, reverse  
188 transcription, amplicon amplification, library preparation, and sequencing, followed by  
189 bioinformatic analysis. As a negative control, nuclease-free water was processed identically,  
190 except for RNA extraction. The sequencing results showed that nearly all reads (98.5%~100%)  
191 were accurately identified as either Wild Type or Omicron BA.4&5 strains across all four mock  
192 communities. The estimated relative abundances for each variant in the mock communities  
193 were 6.7%:92.3%, 21.9%:76.6%, 51.3%:47.5%, and 93.1%:6.9% (**Figure 1B**), closely matching  
194 the original mixing ratios with a deviation range of -3.1% to 3.1%. These results demonstrate  
195 that the RBD amplicon sequencing method is effective for identifying variants and estimating the  
196 composition and structure of SARS-CoV-2 variants in a sample.

197 Next, we applied the RBD amplicon sequencing approach to weekly wastewater samples  
198 collected from the three wastewater treatment plants. All samples tested positive for SARS-  
199 CoV-2. Consistent with clinically reported case data, viral load results revealed three major  
200 waves of infection in the city: from April 2022 to September 2022, from November 2022 to  
201 December 2022, and from February 2023 to the end of the experiment period (August 2023)  
202 (**Figure 1C and Figure S1**).

203 Across the 216 samples analyzed, 91 SARS-CoV-2 variants were identified, each with over  
204 99% identity to the reported variant sequences. For visualization, we plotted the related  
205 abundance of the variants of interest (VOIs) listed by WHO and those with an abundance of  
206 10% or higher in at least one wastewater sample. All other variants were grouped under 'others'.  
207 **Figures 1D-F** show the relative abundance of SARS-CoV-2 variants over the 17 months across  
208 the three sewersheds, highlighting the evolving composition of variant communities. Overall,  
209 each wastewater sample contained multiple variants, and we observed waves of dominant  
210 variants transitioning from BA.2 to BA.2.12.1, BA.4&5, BQ.1, and to XBB.1.5. While there were  
211 some differences, the overall variant profiles for each WWTP were similar, indicating that the  
212 spread and evolution of the virus followed a comparable trajectory across the three sewersheds

213 in the city. These results demonstrate that RBD amplicon sequencing of wastewater samples  
214 can be used to monitor the temporal dynamics and community structure of SARS-CoV-2  
215 variants circulating in the population.

216

### 217 **3.2 Consistency and novel insights from RBD amplicon sequencing data compared to** 218 **clinical genome sequencing data.**

219 We further validated the wastewater findings using reported clinical genome sequencing data  
220 from the USA, Texas, and El Paso. As shown in **Figure 1G**, the overall trends between the  
221 wastewater RBD amplicon sequencing data and clinical genome sequence data in Texas are  
222 consistent, with multiple waves of major variants emerging sequentially. Moreover, the  
223 composition of variants in wastewater samples is more diverse, suggesting that some variants  
224 circulating in the city may go undetected in clinical testing. We further compared the temporal  
225 dynamics of major variants during the study period: BA.2, BA.2.12.1, BA.4&5, BQ.1, and  
226 XBB.1.5 (**Figure 2**) in both wastewater and clinical sequencing data at the El Paso, Texas, and  
227 national levels. All five variant waves were consistently found in both datasets, showing similar  
228 transmission waves and relative abundance at the peaks. We also noticed some differences  
229 between Texas and national trends. For example, the BA.2 peak occurred later, and the BA.4&5  
230 peak arrived earlier and lasted longer in Texas compared to the national data. However,  
231 wastewater data in El Paso closely matched the clinical sequencing data in Texas.

232 In addition, we found that some variants circulated in the population earlier than their prevalence  
233 observed in clinical tests. For example, the XBB.1.5 wave began in December 2022, as shown  
234 in both clinical and wastewater data (Figure 2). However, this variant was detectable in  
235 wastewater samples before the major wave, with small peaks observed in March and  
236 September 2022 (**Figure 2**). Similarly, the waves of EG.5.1 and XBB.1.16 started in May and  
237 March 2023, respectively (**Figure 3A and 3B**), yet these variants were detectable from the  
238 beginning of our experiment. These findings strengthen the existing idea that wastewater  
239 surveillance could provide early warnings to the community<sup>28,46,47</sup>.

240 We also identified some uncommon variants that were not detected in the clinical data. Those  
241 variants, including EF.1.1, GD.1, EG.6.1, and FE.1.2, were barely noticeable in clinical records  
242 due to low abundance but were significant enough to exceed 10% in at least one wastewater  
243 sample (**Figure 3C and 3D, and Figure S2**). The EF.1.1 variant even had a small outbreak in  
244 all of the three sewersheds, with a relative abundance of up to 25% from October 2022 to



245 February 2023. The EG.6.1, FE.1.2, and GD.1 variants were detected throughout the  
246 experiment period, but very few records were found in clinical data. This discrepancy likely  
247 occurs because these variants have a moderate transmission rate but do not cause severe  
248 symptoms, leading to fewer clinical tests.

249 In summary, the results from RBD amplicon sequencing of wastewater samples are consistent  
250 with clinical genome sequencing data in capturing the variants' dynamics. This consistency  
251 highlights the effectiveness and accuracy of this approach in monitoring SARS-CoV-2 variants  
252 circulating in the sewershed. Additionally, the method allows for the early detection of emerging  
253 variants and provides a comprehensive view of variant diversity, emphasizing its importance for  
254 community-level surveillance efforts.

255

### 256 **3.3 RBD amplicon sequencing data highlights off-season and lag-phase as crucial** 257 **periods for variant emergency and evolution.**

258 To better understand the epidemiological dynamics of SARS-CoV-2, we performed alpha  
259 diversity analyses of the variants identified from the RBD amplicon sequencing of wastewater  
260 samples. Specifically, we examined how variant diversity changes with the seasons, during high  
261 transmission periods (in outbreak waves) versus low transmission periods (out of wave), and  
262 across different outbreak phases including lag, growth, stationary, and decline. Metrics including  
263 Observed, Chao1, Shannon, and Inverse Simpson indices were used to measure the richness  
264 and evenness of SARS-CoV-2 variants in the wastewater samples. The Observed index counts  
265 the actual number of unique variants, Chao1 estimates total species richness, Shannon  
266 quantifies the diversity considering both abundance and evenness, and Inverse Simpson  
267 emphasizes the dominance of the most abundant variants.

268 Results revealed significant seasonal variations in alpha diversity in all four metrics (**Figure 4A**).  
269 An increasing trend of alpha diversity was observed from spring to winter, with the highest alpha  
270 diversity observed in winter, suggesting that many variants emerged during the winter months.  
271 And summer months exhibited the lowest diversity. Moreover, higher diversity was also  
272 observed during the low transmission (out of wave) period across the four metrics (**Figure 4B**  
273 **and 4C**). This suggests that during these low transmission periods, a more diverse pool of  
274 variants circulates at low levels in the population, potentially due to reduced selective pressures  
275 compared to the outbreak period. When grouping data into different outbreak phases, we found  
276 that the highest diversity emerged in the lag phase, followed by the decline and growth phases,

277 with the lowest diversity observed in the stationary phase (**Figure 4D and 4E**). This result  
278 suggests an interesting phenomenon: new variants mostly emerged not during the stationary  
279 phase, where the highest viral shedding and new cases occur, but in the lag phase, before a  
280 new outbreak starts. Beta diversity analysis showed no significant difference across the three  
281 sewersheds (**Figure 4F**). Together, these results showed that RBD amplicon sequencing of  
282 wastewater is a powerful tool for uncovering the patterns of variant emergence and evolution in  
283 the sewershed.

284

## 285 **Discussion**

286 One significant insight from this study is the ability of RBD amplicon sequencing data to reveal  
287 patterns of viral evolution and variant emergence. Previous studies using whole genome  
288 sequencing of SARS-CoV-2 in wastewater have highlighted the early-warning potential of this  
289 approach and its ability to uncover variant dynamics<sup>48-51</sup>. However, our study emphasizes that  
290 wastewater data can also be viewed from an ecological and evolutionary perspective, reflecting  
291 the community's viral variant landscape.

292 Our seasonal analysis revealed significant variations in alpha diversity, with higher diversity  
293 observed in winter and lower diversity in summer. This suggests that colder months facilitate the  
294 emergence and spread of more variants, likely due to increased indoor activities, enhanced viral  
295 stability, and seasonal variations in immune responses. Additionally, higher alpha diversity  
296 during low transmission periods and the lag phase of outbreaks indicates that a diverse pool of  
297 variants circulates at low levels during these times. These periods allow for the accumulation  
298 and persistence of a wider range of variants, which may not immediately lead to outbreaks but  
299 could contribute to future waves if conditions become favorable. Ecologically, the lag phase  
300 represents a period of low competition, allowing new variants to compete until a strain with the  
301 highest fitness prevails. These insights underscore the importance of continuous monitoring of  
302 viral diversity to predict future outbreaks and implement timely public health interventions.

303 Our findings also demonstrate that RBD amplicon sequencing of wastewater samples effectively  
304 captures the dynamics of SARS-CoV-2 variants, showing consistent results with clinical genome  
305 sequencing data at local, state, and national levels. Notably, our study identified variants  
306 circulating in the population earlier than observed in clinical sequencing data and detected  
307 variants and outbreaks that were not reported or noticed locally. This consistency with clinical  
308 genome sequencing data and the earlier detection of variants underscore the accuracy and

309 reliability of RBD amplicon sequencing of wastewater in variant surveillance. It also strengthens  
310 the role of wastewater surveillance as a complementary tool to clinical testing<sup>24–26,52–55</sup>,  
311 especially valuable in areas with limited access to clinical sequencing resources.

312 Despite its advantages, RBD amplicon sequencing has limitations. While the RBD region is rich  
313 in information and useful for targeted analysis, it represents only a small portion of the viral  
314 genome. This limitation means that mutations outside the RBD region will be missed, and  
315 closely related variants with mutations in other regions may not be differentiated. Additionally,  
316 evolutionary changes occurring outside the targeted region, including recombination events, are  
317 not captured. The PCR amplification step can also introduce biases<sup>56–58</sup>, potentially skewing the  
318 relative abundance of certain variants. While our analyses using synthetic variant communities  
319 (**Figure 1B**) suggest that this bias may not significantly impact our results, further validation is  
320 necessary. On the other hand, RBD amplicon sequencing is faster, easier, and cheaper than  
321 whole genome sequencing<sup>20,59,60</sup>, making it accessible for widespread use. Its high throughput  
322 capability with relatively lower costs allows for the rapid analysis of numerous samples, which is  
323 critical during pandemic conditions. By balancing these trade-offs, RBD amplicon sequencing  
324 provides a practical and efficient tool for ongoing variant surveillance, particularly when rapid  
325 data collection is necessary and resources are constrained.

326 Viruses have various mechanisms to enhance transmission between hosts. One significant  
327 strategy is mutating the receptor-binding domain in the spike gene, as observed with SARS-  
328 CoV-2, which has produced multiple waves of variants from Alpha to Omicron. These mutations  
329 in RBD enable the virus to evade adaptive immune responses from prior infections and/or  
330 vaccinations. Consequently, monitoring the RBD region is crucial for tracking viral evolution,  
331 predicting the emergence of new variants, and informing updated vaccine composition. This  
332 study highlights the utility of RBD amplicon sequencing and the integration of wastewater  
333 surveillance to track SARS-CoV-2 evolution and variant emergence. Our findings demonstrate  
334 that this tool captures the dynamics of variant community, provides early detection of variants,  
335 aligns well with clinical genome sequencing data, and reveals epidemiological patterns in viral  
336 diversity. The concept of monitoring the receptor-binding domain can also be generalized to  
337 other viruses, providing a broader framework for variant surveillance. This tool can improve our  
338 ability to predict future outbreaks and enhance public health preparedness.

339

340 **Declaration of Competing Interest**

341 The authors declare no competing interest.

342

### 343 **Data and Code Availability**

344 Data in this study will be shared with the paper publication. Scripts will be shared on GitHub.

345

### 346 **Acknowledgments**

347 We are grateful to Teresa T. Alcalá at El Paso Water for sample collection and shipping. This  
348 work is supported by the PRIME award from the UTHealth Houston School of Public Health,  
349 National Institute of Health RADxUP (1U01TR004355-01), and the Texas Epidemic Public  
350 Health Institute (TEPHI).

351

### 352 **References**

- 353 (1) Shin, H. J.; Ku, K. B.; Kim, H. S.; Moon, H. W.; Jeong, G. U.; Hwang, I.; Yoon, G. Y.; Lee, S.; Lee, S.;  
354 Ahn, D.-G.; Kim, K.-D.; Kwon, Y.-C.; Kim, B.-T.; Kim, S.-J.; Kim, C. Receptor-Binding Domain of SARS-  
355 CoV-2 Spike Protein Efficiently Inhibits SARS-CoV-2 Infection and Attachment to Mouse Lung. *Int. J.*  
356 *Biol. Sci.* **2021**, *17* (14), 3786–3794. <https://doi.org/10.7150/ijbs.61320>.
- 357 (2) Tai, W.; He, L.; Zhang, X.; Pu, J.; Voronin, D.; Jiang, S.; Zhou, Y.; Du, L. Characterization of the  
358 Receptor-Binding Domain (RBD) of 2019 Novel Coronavirus: Implication for Development of RBD  
359 Protein as a Viral Attachment Inhibitor and Vaccine. *Cell. Mol. Immunol.* **2020**, *17* (6), 613–620.  
360 <https://doi.org/10.1038/s41423-020-0400-4>.
- 361 (3) Shang, J.; Wan, Y.; Luo, C.; Ye, G.; Geng, Q.; Auerbach, A.; Li, F. Cell Entry Mechanisms of SARS-CoV-  
362 2. *Proc. Natl. Acad. Sci.* **2020**, *117* (21), 11727–11734. <https://doi.org/10.1073/pnas.2003138117>.
- 363 (4) Chakraborty, C.; Bhattacharya, M.; Sharma, A. R. Present Variants of Concern and Variants of  
364 Interest of Severe Acute Respiratory Syndrome Coronavirus 2: Their Significant Mutations in S-  
365 Glycoprotein, Infectivity, Re-Infectivity, Immune Escape and Vaccines Activity. *Rev. Med. Virol.*  
366 **2022**, *32* (2), e2270. <https://doi.org/10.1002/rmv.2270>.
- 367 (5) Dhawan, M.; Sharma, A.; Priyanka; Thakur, N.; Rajkhowa, T. K.; Choudhary, O. P. Delta Variant  
368 (B.1.617.2) of SARS-CoV-2: Mutations, Impact, Challenges and Possible Solutions. *Hum. Vaccines*  
369 *Immunother.* *18* (5), 2068883. <https://doi.org/10.1080/21645515.2022.2068883>.
- 370 (6) Adhikari, P.; Jawad, B.; Rao, P.; Podgornik, R.; Ching, W.-Y. Delta Variant with P681R Critical  
371 Mutation Revealed by Ultra-Large Atomic-Scale Ab Initio Simulation: Implications for the  
372 Fundamentals of Biomolecular Interactions. *Viruses* **2022**, *14* (3), 465.  
373 <https://doi.org/10.3390/v14030465>.
- 374 (7) Bhattacharya, M.; Chatterjee, S.; Sharma, A. R.; Lee, S.-S.; Chakraborty, C. Delta Variant (B.1.617.2)  
375 of SARS-CoV-2: Current Understanding of Infection, Transmission, Immune Escape, and Mutational  
376 Landscape. *Folia Microbiol. (Praha)* **2023**, *68* (1), 17–28. [https://doi.org/10.1007/s12223-022-](https://doi.org/10.1007/s12223-022-01001-3)  
377 01001-3.

- 378 (8) Goher, S. S.; Ali, F.; Amin, M. The Delta Variant Mutations in the Receptor Binding Domain of SARS-  
379 CoV-2 Show Enhanced Electrostatic Interactions with the ACE2. *Med. Drug Discov.* **2022**, *13*,  
380 100114. <https://doi.org/10.1016/j.medidd.2021.100114>.
- 381 (9) Pondé, R. A. A. Physicochemical Effect of the N501Y, E484K/Q, K417N/T, L452R and T478K  
382 Mutations on the SARS-CoV-2 Spike Protein RBD and Its Influence on Agent Fitness and on  
383 Attributes Developed by Emerging Variants of Concern. *Virology* **2022**, *572*, 44–54.  
384 <https://doi.org/10.1016/j.virol.2022.05.003>.
- 385 (10) Schwarze, K.; Buchanan, J.; Taylor, J. C.; Wordsworth, S. Are Whole-Exome and Whole-Genome  
386 Sequencing Approaches Cost-Effective? A Systematic Review of the Literature. *Genet. Med.* **2018**,  
387 *20* (10), 1122–1130. <https://doi.org/10.1038/gim.2017.247>.
- 388 (11) Christensen, K. D.; Dukhovny, D.; Siebert, U.; Green, R. C. Assessing the Costs and Cost-  
389 Effectiveness of Genomic Sequencing. *J. Pers. Med.* **2015**, *5* (4), 470–486.  
390 <https://doi.org/10.3390/jpm5040470>.
- 391 (12) Nurchis, M. C.; Riccardi, M. T.; Damiani, G. Health Technology Assessment of Whole Genome  
392 Sequencing in the Diagnosis of Genetic Disorders: A Scoping Review of the Literature. *Int. J.*  
393 *Technol. Assess. Health Care* **2022**, *38* (1), e71. <https://doi.org/10.1017/S0266462322000496>.
- 394 (13) Long, Q.-X.; Tang, X.-J.; Shi, Q.-L.; Li, Q.; Deng, H.-J.; Yuan, J.; Hu, J.-L.; Xu, W.; Zhang, Y.; Lv, F.-J.; Su,  
395 K.; Zhang, F.; Gong, J.; Wu, B.; Liu, X.-M.; Li, J.-J.; Qiu, J.-F.; Chen, J.; Huang, A.-L. Clinical and  
396 Immunological Assessment of Asymptomatic SARS-CoV-2 Infections. *Nat. Med.* **2020**, *26* (8), 1200–  
397 1204. <https://doi.org/10.1038/s41591-020-0965-6>.
- 398 (14) Sah, P.; Fitzpatrick, M. C.; Zimmer, C. F.; Abdollahi, E.; Juden-Kelly, L.; Moghadas, S. M.; Singer, B.  
399 H.; Galvani, A. P. Asymptomatic SARS-CoV-2 Infection: A Systematic Review and Meta-Analysis.  
400 *Proc. Natl. Acad. Sci. U. S. A.* **2021**, *118* (34), e2109229118.  
401 <https://doi.org/10.1073/pnas.2109229118>.
- 402 (15) You, Y.; Yang, X.; Hung, D.; Yang, Q.; Wu, T.; Deng, M. Asymptomatic COVID-19 Infection:  
403 Diagnosis, Transmission, Population Characteristics. *BMJ Support. Palliat. Care* **2024**, *14* (e1),  
404 e220–e227. <https://doi.org/10.1136/bmjspcare-2020-002813>.
- 405 (16) Kimball, A. Asymptomatic and Presymptomatic SARS-CoV-2 Infections in Residents of a Long-Term  
406 Care Skilled Nursing Facility — King County, Washington, March 2020. *MMWR Morb. Mortal. Wkly.*  
407 *Rep.* **2020**, *69*. <https://doi.org/10.15585/mmwr.mm6913e1>.
- 408 (17) Thompson, J. R.; Nancharaiah, Y. V.; Gu, X.; Lee, W. L.; Rajal, V. B.; Haines, M. B.; Girones, R.; Ng, L.  
409 C.; Alm, E. J.; Wuertz, S. Making Waves: Wastewater Surveillance of SARS-CoV-2 for Population-  
410 Based Health Management. *Water Res.* **2020**, *184*, 116181.  
411 <https://doi.org/10.1016/j.watres.2020.116181>.
- 412 (18) Xagorarakis, I. Can We Predict Viral Outbreaks Using Wastewater Surveillance? *J. Environ. Eng.*  
413 **2020**, *146* (11), 01820003. [https://doi.org/10.1061/\(ASCE\)EE.1943-7870.0001831](https://doi.org/10.1061/(ASCE)EE.1943-7870.0001831).
- 414 (19) Kilaru, P.; Hill, D.; Anderson, K.; Collins, M. B.; Green, H.; Kmush, B. L.; Larsen, D. A. Wastewater  
415 Surveillance for Infectious Disease: A Systematic Review. *Am. J. Epidemiol.* **2023**, *192* (2), 305–322.  
416 <https://doi.org/10.1093/aje/kwac175>.
- 417 (20) Kuroiwa, M.; Gahara, Y.; Kato, H.; Morikawa, Y.; Matsui, Y.; Adachi, T.; Kurosawa, S.; Kuroita, T.;  
418 Ando, Y.; Rokushima, M. Targeted Amplicon Sequencing of Wastewater Samples for Detecting  
419 SARS-CoV-2 Variants with High Sensitivity and Resolution. *Sci. Total Environ.* **2023**, *893*, 164766.  
420 <https://doi.org/10.1016/j.scitotenv.2023.164766>.
- 421 (21) Iwamoto, R.; Yamaguchi, K.; Katayama, K.; Ando, H.; Setsukinai, K.; Kobayashi, H.; Okabe, S.; Imoto,  
422 S.; Kitajima, M. Identification of SARS-CoV-2 Variants in Wastewater Using Targeted Amplicon  
423 Sequencing during a Low COVID-19 Prevalence Period in Japan. *Sci. Total Environ.* **2023**, *887*,  
424 163706. <https://doi.org/10.1016/j.scitotenv.2023.163706>.

- 425 (22) Lou, E. G.; Sapoval, N.; McCall, C.; Bauhs, L.; Carlson-Stadler, R.; Kalvapalle, P.; Lai, Y.; Palmer, K.;  
426 Penn, R.; Rich, W.; Wolken, M.; Brown, P.; Ensor, K. B.; Hopkins, L.; Treangen, T. J.; Stadler, L. B.  
427 Direct Comparison of RT-ddPCR and Targeted Amplicon Sequencing for SARS-CoV-2 Mutation  
428 Monitoring in Wastewater. *Sci. Total Environ.* **2022**, *833*, 155059.  
429 <https://doi.org/10.1016/j.scitotenv.2022.155059>.
- 430 (23) *Environmental surveillance for SARS-COV-2 to complement public health surveillance – Interim*  
431 *Guidance*. <https://www.who.int/publications/i/item/WHO-HEP-ECH-WSH-2022.1> (accessed 2024-  
432 06-26).
- 433 (24) Bisseux, M.; Debroas, D.; Mirand, A.; Archimbaud, C.; Peigue-Lafeuille, H.; Bailly, J.-L.; Henquell, C.  
434 Monitoring of Enterovirus Diversity in Wastewater by Ultra-Deep Sequencing: An Effective  
435 Complementary Tool for Clinical Enterovirus Surveillance. *Water Res.* **2020**, *169*, 115246.  
436 <https://doi.org/10.1016/j.watres.2019.115246>.
- 437 (25) Fantilli, A.; Cola, G. D.; Castro, G.; Sicilia, P.; Cachi, A. M.; de los Ángeles Marinzalda, M.; Ibarra, G.;  
438 López, L.; Valdivino, C.; Barbás, G.; Nates, S.; Masachessi, G.; Pisano, M. B.; Ré, V. Hepatitis A Virus  
439 Monitoring in Wastewater: A Complementary Tool to Clinical Surveillance. *Water Res.* **2023**, *241*,  
440 120102. <https://doi.org/10.1016/j.watres.2023.120102>.
- 441 (26) Smith, T.; Holm, R. H.; Yeager, R.; Moore, J. B.; Rouchka, E. C.; Sokoloski, K. J.; Elliott, E. M.; Talley,  
442 D.; Arora, V.; Moyer, S.; Bhatnagar, A. Combining Community Wastewater Genomic Surveillance  
443 with State Clinical Surveillance: A Framework for SARS-CoV-2 Public Health Practice. *Food Environ.*  
444 *Virol.* **2022**, *14* (4), 410–416. <https://doi.org/10.1007/s12560-022-09531-2>.
- 445 (27) Li, J.; Hosegood, I.; Powell, D.; Tschärke, B.; Lawler, J.; Thomas, K. V.; Mueller, J. F. A Global  
446 Aircraft-Based Wastewater Genomic Surveillance Network for Early Warning of Future Pandemics.  
447 *Lancet Glob. Health* **2023**, *11* (5), e791–e795. [https://doi.org/10.1016/S2214-109X\(23\)00129-8](https://doi.org/10.1016/S2214-109X(23)00129-8).
- 448 (28) Karthikeyan, S.; Levy, J. I.; De Hoff, P.; Humphrey, G.; Birmingham, A.; Jepsen, K.; Farmer, S.; Tubb,  
449 H. M.; Valles, T.; Tribelhorn, C. E.; Tsai, R.; Aigner, S.; Sathe, S.; Moshiri, N.; Henson, B.; Mark, A.  
450 M.; Hakim, A.; Baer, N. A.; Barber, T.; Belda-Ferre, P.; Chacón, M.; Cheung, W.; Cresini, E. S.; Eisner,  
451 E. R.; Lastrella, A. L.; Lawrence, E. S.; Marotz, C. A.; Ngo, T. T.; Ostrander, T.; Plascencia, A.; Salido,  
452 R. A.; Seaver, P.; Smoot, E. W.; McDonald, D.; Neuhard, R. M.; Scioscia, A. L.; Satterlund, A. M.;  
453 Simmons, E. H.; Abelman, D. B.; Brenner, D.; Bruner, J. C.; Buckley, A.; Ellison, M.; Gattas, J.;  
454 Gonias, S. L.; Hale, M.; Hawkins, F.; Ikeda, L.; Jhaveri, H.; Johnson, T.; Kellen, V.; Kremer, B.;  
455 Matthews, G.; McLawhon, R. W.; Ouillet, P.; Park, D.; Pradenas, A.; Reed, S.; Riggs, L.; Sanders, A.;  
456 Sollenberger, B.; Song, A.; White, B.; Winbush, T.; Aceves, C. M.; Anderson, C.; Gangavarapu, K.;  
457 Hufbauer, E.; Kurzban, E.; Lee, J.; Matteson, N. L.; Parker, E.; Perkins, S. A.; Ramesh, K. S.; Robles-  
458 Sikisaka, R.; Schwab, M. A.; Spencer, E.; Wohl, S.; Nicholson, L.; McHardy, I. H.; Dimmock, D. P.;  
459 Hobbs, C. A.; Bakhtar, O.; Harding, A.; Mendoza, A.; Bolze, A.; Becker, D.; Cirulli, E. T.; Isaksson, M.;  
460 Schiabor Barrett, K. M.; Washington, N. L.; Malone, J. D.; Schafer, A. M.; Gurfield, N.; Stous, S.;  
461 Fielding-Miller, R.; Garfein, R. S.; Gaines, T.; Anderson, C.; Martin, N. K.; Schooley, R.; Austin, B.;  
462 MacCannell, D. R.; Kingsmore, S. F.; Lee, W.; Shah, S.; McDonald, E.; Yu, A. T.; Zeller, M.; Fisch, K.  
463 M.; Longhurst, C.; Maysent, P.; Pride, D.; Khosla, P. K.; Laurent, L. C.; Yeo, G. W.; Andersen, K. G.;  
464 Knight, R. Wastewater Sequencing Reveals Early Cryptic SARS-CoV-2 Variant Transmission. *Nature*  
465 **2022**, *609* (7925), 101–108. <https://doi.org/10.1038/s41586-022-05049-6>.
- 466 (29) Jiang, M.; Wang, A. L. W.; Be, N. A.; Mulakken, N.; Nelson, K. L.; Kantor, R. S. Evaluation of the  
467 Impact of Concentration and Extraction Methods on the Targeted Sequencing of Human Viruses  
468 from Wastewater. *Environ. Sci. Technol.* **2024**, *58* (19), 8239–8250.  
469 <https://doi.org/10.1021/acs.est.4c00580>.
- 470 (30) Levy, J. I.; Andersen, K. G.; Knight, R.; Karthikeyan, S. Wastewater Surveillance for Public Health.  
471 *Science* **2023**, *379* (6627), 26–27. <https://doi.org/10.1126/science.ade2503>.

- 472 (31) Parkins, M. D.; Lee, B. E.; Acosta, N.; Bautista, M.; Hubert, C. R. J.; Hrudey, S. E.; Frankowski, K.;  
473 Pang, X.-L. Wastewater-Based Surveillance as a Tool for Public Health Action: SARS-CoV-2 and  
474 Beyond. *Clin. Microbiol. Rev.* **2023**, *37* (1), e00103-22. <https://doi.org/10.1128/cmr.00103-22>.
- 475 (32) Li, Y.; Miyani, B.; Childs, K. L.; Shiu, S.-H.; Xagorarakis, I. Effect of Wastewater Collection and  
476 Concentration Methods on Assessment of Viral Diversity. *Sci. Total Environ.* **2024**, *908*, 168128.  
477 <https://doi.org/10.1016/j.scitotenv.2023.168128>.
- 478 (33) Gregory, D. A.; Trujillo, M.; Rushford, C.; Flury, A.; Kannoly, S.; San, K. M.; Lyfoung, D. T.; Wiseman,  
479 R. W.; Bromert, K.; Zhou, M.-Y.; Kesler, E.; Bivens, N. J.; Hoskins, J.; Lin, C.-H.; O'Connor, D. H.;  
480 Wieberg, C.; Wenzel, J.; Kantor, R. S.; Dennehy, J. J.; Johnson, M. C. Genetic Diversity and  
481 Evolutionary Convergence of Cryptic SARS-CoV-2 Lineages Detected via Wastewater Sequencing.  
482 *PLoS Pathog.* **2022**, *18* (10), e1010636. <https://doi.org/10.1371/journal.ppat.1010636>.
- 483 (34) Baaijens, J. A.; Zulli, A.; Ott, I. M.; Nika, I.; van der Lugt, M. J.; Petrone, M. E.; Alpert, T.; Fauver, J.  
484 R.; Kalinich, C. C.; Vogels, C. B. F.; Breban, M. I.; Duvallet, C.; McElroy, K. A.; Ghaeli, N.; Imakaev,  
485 M.; McKenzie-Bennett, M. F.; Robison, K.; Plocik, A.; Schilling, R.; Pierson, M.; Littlefield, R.;  
486 Spencer, M. L.; Simen, B. B.; Altajar, A.; Brito, A. F.; Watkins, A. E.; Muyombwe, A.; Neal, C.; Liu, C.;  
487 Castaldi, C.; Pearson, C.; Peaper, D. R.; Laszlo, E.; Tikhonova, I. R.; Razeq, J.; Rothman, J. E.; Wang,  
488 J.; Bilguvar, K.; Niccolai, L.; Wilson, M. S.; Anderson, M. L.; Landry, M. L.; Adams, M. D.; Hui, P.;  
489 Downing, R.; Earnest, R.; Mane, S.; Murphy, S.; Hanage, W. P.; Grubaugh, N. D.; Peccia, J.; Baym,  
490 M.; Yale SARS-CoV-2 Genomic Surveillance Initiative. Lineage Abundance Estimation for SARS-CoV-  
491 2 in Wastewater Using Transcriptome Quantification Techniques. *Genome Biol.* **2022**, *23* (1), 236.  
492 <https://doi.org/10.1186/s13059-022-02805-9>.
- 493 (35) Cancela, F.; Ramos, N.; Smyth, D. S.; Etchebehere, C.; Berois, M.; Rodríguez, J.; Rufo, C.; Alemán,  
494 A.; Borzacconi, L.; López, J.; González, E.; Botto, G.; Thornhill, S. G.; Mirazo, S.; Trujillo, M.  
495 Wastewater Surveillance of SARS-CoV-2 Genomic Populations on a Country-Wide Scale through  
496 Targeted Sequencing. *PLOS ONE* **2023**, *18* (4), e0284483.  
497 <https://doi.org/10.1371/journal.pone.0284483>.
- 498 (36) Gregory, D. A.; Wieberg, C. G.; Wenzel, J.; Lin, C.-H.; Johnson, M. C. Monitoring SARS-CoV-2  
499 Populations in Wastewater by Amplicon Sequencing and Using the Novel Program SAM Refiner.  
500 *Viruses* **2021**, *13* (8), 1647. <https://doi.org/10.3390/v13081647>.
- 501 (37) Adamopoulos, P. G.; Diamantopoulos, M. A.; Boti, M. A.; Zafeiriadou, A.; Galani, A.; Kostakis, M.;  
502 Markou, A.; Sideris, D. C.; Avgeris, M.; Thomaidis, N. S.; Scorilas, A. Spike-Seq: An Amplicon-Based  
503 High-Throughput Sequencing Approach for the Sensitive Detection and Characterization of SARS-  
504 CoV-2 Genetic Variations in Environmental Samples. *Sci. Total Environ.* **2024**, *914*, 169747.  
505 <https://doi.org/10.1016/j.scitotenv.2023.169747>.
- 506 (38) Rodrigues, G. M.; Volpato, F. C. Z.; Wink, P. L.; Paiva, R. M.; Barth, A. L.; de-Paris, F. SARS-CoV-2  
507 Variants of Concern: Presumptive Identification via Sanger Sequencing Analysis of the Receptor  
508 Binding Domain (RBD) Region of the S Gene. *Diagnostics* **2023**, *13* (7), 1256.  
509 <https://doi.org/10.3390/diagnostics13071256>.
- 510 (39) Oghuan, J.; Chavarria, C.; Vanderwal, S. R.; Gitter, A.; Ojaruega, A. A.; Monserrat, C.; Bauer, C. X.;  
511 Brown, E. L.; Cregeen, S. J.; Deegan, J.; Hanson, B. M.; Tisza, M.; Ocaranza, H. I.; Balliew, J.;  
512 Maresso, A. W.; Rios, J.; Boerwinkle, E.; Mena, K. D.; Wu, F. Wastewater Analysis of Mpox Virus in  
513 a City with Low Prevalence of Mpox Disease: An Environmental Surveillance Study. *Lancet Reg.*  
514 *Health – Am.* **2023**, *28*. <https://doi.org/10.1016/j.lana.2023.100639>.
- 515 (40) Wu, F.; Xiao, A.; Zhang, J.; Moniz, K.; Endo, N.; Armas, F.; Bonneau, R.; Brown, M. A.; Bushman, M.;  
516 Chai, P. R.; Duvallet, C.; Erickson, T. B.; Foppe, K.; Ghaeli, N.; Gu, X.; Hanage, W. P.; Huang, K. H.;  
517 Lee, W. L.; Matus, M.; McElroy, K. A.; Nagler, J.; Rhode, S. F.; Santillana, M.; Tucker, J. A.; Wuertz,  
518 S.; Zhao, S.; Thompson, J.; Alm, E. J. SARS-CoV-2 RNA Concentrations in Wastewater Foreshadow

- 519 Dynamics and Clinical Presentation of New COVID-19 Cases. *Sci. Total Environ.* **2022**, *805*, 150121.  
520 <https://doi.org/10.1016/j.scitotenv.2021.150121>.
- 521 (41) Wu, F.; Xiao, A.; Zhang, J.; Moniz, K.; Endo, N.; Armas, F.; Bushman, M.; Chai, P. R.; Duvallet, C.;  
522 Erickson, T. B.; Foppe, K.; Ghaeli, N.; Gu, X.; Hanage, W. P.; Huang, K. H.; Lee, W. L.; McElroy, K. A.;  
523 Rhode, S. F.; Matus, M.; Wuertz, S.; Thompson, J.; Alm, E. J. Wastewater Surveillance of SARS-CoV-  
524 2 across 40 U.S. States from February to June 2020. *Water Res.* **2021**, *202*, 117400.  
525 <https://doi.org/10.1016/j.watres.2021.117400>.
- 526 (42) Wu, F.; Xiao, A.; Zhang, J.; Gu, X.; Lee, W. L.; Kauffman, K.; Hanage, W.; Matus, M.; Ghaeli, N.;  
527 Endo, N.; Duvallet, C.; Moniz, K.; Erickson, T.; Chai, P.; Thompson, J.; Alm, E. SARS-CoV-2 Titers in  
528 Wastewater Are Higher than Expected from Clinically Confirmed Cases. *mSystems* **2020**, *5* (4),  
529 2020.04.05.20051540. <https://doi.org/10.1128/mSystems.00614-20>.
- 530 (43) Callahan, B. J.; McMurdie, P. J.; Rosen, M. J.; Han, A. W.; Johnson, A. J. A.; Holmes, S. P. DADA2:  
531 High-Resolution Sample Inference from Illumina Amplicon Data. *Nat. Methods* **2016**, *13* (7), 581–  
532 583. <https://doi.org/10.1038/nmeth.3869>.
- 533 (44) Sayers, E. W.; Bolton, E. E.; Brister, J. R.; Canese, K.; Chan, J.; Comeau, D. C.; Connor, R.; Funk, K.;  
534 Kelly, C.; Kim, S.; Madej, T.; Marchler-Bauer, A.; Lanczycki, C.; Lathrop, S.; Lu, Z.; Thibaud-Nissen, F.;  
535 Murphy, T.; Phan, L.; Skripchenko, Y.; Tse, T.; Wang, J.; Williams, R.; Trawick, B. W.; Pruitt, K. D.;  
536 Sherry, S. T. Database Resources of the National Center for Biotechnology Information. *Nucleic  
537 Acids Res.* **2021**, *50* (D1), D20–D26. <https://doi.org/10.1093/nar/gkab1112>.
- 538 (45) Wirth, W.; Duchene, S. GISAIDR, 2022. <https://doi.org/10.5281/zenodo.6474693>.
- 539 (46) Amman, F.; Markt, R.; Endler, L.; Hupfau, S.; Agerer, B.; Schedl, A.; Richter, L.; Zechmeister, M.;  
540 Bicher, M.; Heiler, G.; Triska, P.; Thornton, M.; Penz, T.; Senekowitsch, M.; Laine, J.; Keszei, Z.;  
541 Klimek, P.; Nägele, F.; Mayr, M.; Daleiden, B.; Steinlechner, M.; Niederstätter, H.; Heidinger, P.;  
542 Rauch, W.; Scheffknecht, C.; Vogl, G.; Weichlinger, G.; Wagner, A. O.; Slipko, K.; Masseron, A.;  
543 Radu, E.; Allerberger, F.; Popper, N.; Bock, C.; Schmid, D.; Oberacher, H.; Kreuzinger, N.; Insam, H.;  
544 Bergthaler, A. Viral Variant-Resolved Wastewater Surveillance of SARS-CoV-2 at National Scale.  
545 *Nat. Biotechnol.* **2022**, *40* (12), 1814–1822. <https://doi.org/10.1038/s41587-022-01387-y>.
- 546 (47) Gupta, P.; Liao, S.; Ezekiel, M.; Novak, N.; Rossi, A.; LaCross, N.; Oakeson, K.; Rohrwasser, A.  
547 Wastewater Genomic Surveillance Captures Early Detection of Omicron in Utah. *Microbiol. Spectr.*  
548 **2023**, *11* (3), e00391-23. <https://doi.org/10.1128/spectrum.00391-23>.
- 549 (48) Oude Munnink, B. B.; Nieuwenhuijse, D. F.; Stein, M.; O’Toole, Á.; Haverkate, M.; Mollers, M.;  
550 Kamga, S. K.; Schapendonk, C.; Pronk, M.; Lexmond, P.; van der Linden, A.; Bestebroer, T.;  
551 Chestakova, I.; Overmars, R. J.; van Nieuwkoop, S.; Molenkamp, R.; van der Eijk, A. A.;  
552 GeurtsvanKessel, C.; Vennema, H.; Meijer, A.; Rambaut, A.; van Dissel, J.; Sikkema, R. S.; Timen, A.;  
553 Koopmans, M. Rapid SARS-CoV-2 Whole-Genome Sequencing and Analysis for Informed Public  
554 Health Decision-Making in the Netherlands. *Nat. Med.* **2020**, *26* (9), 1405–1410.  
555 <https://doi.org/10.1038/s41591-020-0997-y>.
- 556 (49) Mao, K.; Zhang, K.; Du, W.; Ali, W.; Feng, X.; Zhang, H. The Potential of Wastewater-Based  
557 Epidemiology as Surveillance and Early Warning of Infectious Disease Outbreaks. *Curr. Opin.  
558 Environ. Sci. Health* **2020**, *17*, 1–7. <https://doi.org/10.1016/j.coesh.2020.04.006>.
- 559 (50) Ahmed, W.; Tschärke, B.; Bertsch, P. M.; Bibby, K.; Bivins, A.; Choi, P.; Clarke, L.; Dwyer, J.; Edson,  
560 J.; Nguyen, T. M. H.; O’Brien, J. W.; Simpson, S. L.; Sherman, P.; Thomas, K. V.; Verhagen, R.; Zaugg,  
561 J.; Mueller, J. F. SARS-CoV-2 RNA Monitoring in Wastewater as a Potential Early Warning System  
562 for COVID-19 Transmission in the Community: A Temporal Case Study. *Sci. Total Environ.* **2021**,  
563 *761*, 144216. <https://doi.org/10.1016/j.scitotenv.2020.144216>.
- 564 (51) Mackulák, T.; Gál, M.; Špalková, V.; Fehér, M.; Briestenská, K.; Mikušová, M.; Tomčíková, K.;  
565 Tamáš, M.; Butor Škulcová, A. Wastewater-Based Epidemiology as an Early Warning System for the

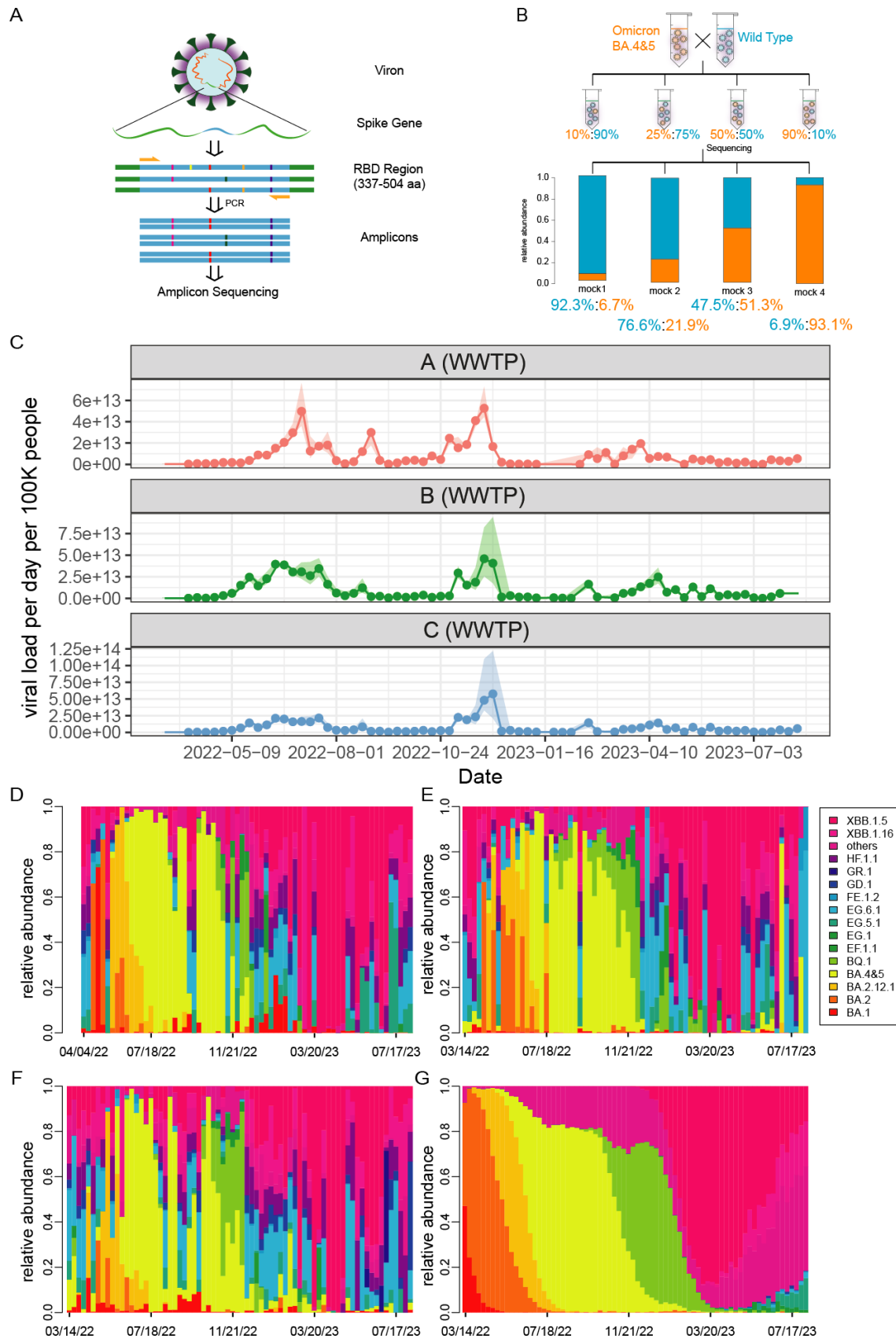


- 566 Spreading of SARS-CoV-2 and Its Mutations in the Population. *Int. J. Environ. Res. Public Health*  
567 **2021**, *18* (11), 5629. <https://doi.org/10.3390/ijerph18115629>.
- 568 (52) Gitter, A.; Oghuan, J.; Godbole, A. R.; Chavarria, C. A.; Monserrat, C.; Hu, T.; Wang, Y.; Maresso, A.  
569 W.; Hanson, B. M.; Mena, K. D.; Wu, F. Not a Waste: Wastewater Surveillance to Enhance Public  
570 Health. *Front. Chem. Eng.* **2023**, *4*. <https://doi.org/10.3389/fceng.2022.1112876>.
- 571 (53) CDC. *About CDC's National Wastewater Surveillance System (NWSS)*. Centers for Disease Control  
572 and Prevention. <https://www.cdc.gov/nwss/about.html> (accessed 2024-06-26).
- 573 (54) DeJonge, P. M.; Adams, C.; Pray, I.; Schussman, M. K.; Fahney, R. B.; Shafer, M.; Antkiewicz, D. S.;  
574 Roguet, A. Wastewater Surveillance Data as a Complement to Emergency Department Visit Data  
575 for Tracking Incidence of Influenza A and Respiratory Syncytial Virus - Wisconsin, August 2022-  
576 March 2023. *MMWR Morb. Mortal. Wkly. Rep.* **2023**, *72* (37), 1005–1009.  
577 <https://doi.org/10.15585/mmwr.mm7237a2>.
- 578 (55) Bonanno Ferraro, G.; Veneri, C.; Mancini, P.; Iaconelli, M.; Suffredini, E.; Bonadonna, L.; Lucentini,  
579 L.; Bowo-Ngandji, A.; Kengne-Nde, C.; Mbaga, D. S.; Mahamat, G.; Tazokong, H. R.; Ebogo-Belobo,  
580 J. T.; Njouom, R.; Kenmoe, S.; La Rosa, G. A State-of-the-Art Scoping Review on SARS-CoV-2 in  
581 Sewage Focusing on the Potential of Wastewater Surveillance for the Monitoring of the COVID-19  
582 Pandemic. *Food Environ. Virol.* **2022**, *14* (4), 315–354. [https://doi.org/10.1007/s12560-021-09498-](https://doi.org/10.1007/s12560-021-09498-6)  
583 [6](https://doi.org/10.1007/s12560-021-09498-6).
- 584 (56) Acinas, S. G.; Sarma-Rupavtarm, R.; Klepac-Ceraj, V.; Polz, M. F. PCR-Induced Sequence Artifacts  
585 and Bias: Insights from Comparison of Two 16S rRNA Clone Libraries Constructed from the Same  
586 Sample. *Appl. Environ. Microbiol.* **2005**, *71* (12), 8966–8969.  
587 <https://doi.org/10.1128/AEM.71.12.8966-8969.2005>.
- 588 (57) Kanagawa, T. Bias and Artifacts in Multitemplate Polymerase Chain Reactions (PCR). *J. Biosci.*  
589 *Bioeng.* **2003**, *96* (4), 317–323. [https://doi.org/10.1016/S1389-1723\(03\)90130-7](https://doi.org/10.1016/S1389-1723(03)90130-7).
- 590 (58) Krehenwinkel, H.; Wolf, M.; Lim, J. Y.; Rominger, A. J.; Simison, W. B.; Gillespie, R. G. Estimating  
591 and Mitigating Amplification Bias in Qualitative and Quantitative Arthropod Metabarcoding. *Sci.*  
592 *Rep.* **2017**, *7* (1), 17668. <https://doi.org/10.1038/s41598-017-17333-x>.
- 593 (59) Techera, C.; Tomás, G.; Grecco, S.; Williman, J.; Hernández, M.; Olivera, V.; Banda, A.; Vagnozzi, A.;  
594 Panzera, Y.; Marandino, A.; Pérez, R. A Rapid and Affordable Amplicon-Based Method for next-  
595 Generation Genome Sequencing of the Infectious Bursal Disease Virus. *J. Virol. Methods* **2023**, *322*,  
596 114807. <https://doi.org/10.1016/j.jviromet.2023.114807>.
- 597 (60) Kong, X.; Gao, P.; Jiang, Y.; Lu, L.; Zhao, M.; Liu, Y.; Deng, G.; Zhu, H.; Cao, Y.; Ma, L. Discrimination  
598 of SARS-CoV-2 Omicron Variant and Its Lineages by Rapid Detection of Immune-Escape Mutations  
599 in Spike Protein RBD Using Asymmetric PCR-Based Melting Curve Analysis. *Virol. J.* **2023**, *20* (1),  
600 192. <https://doi.org/10.1186/s12985-023-02137-5>.

601

602

603

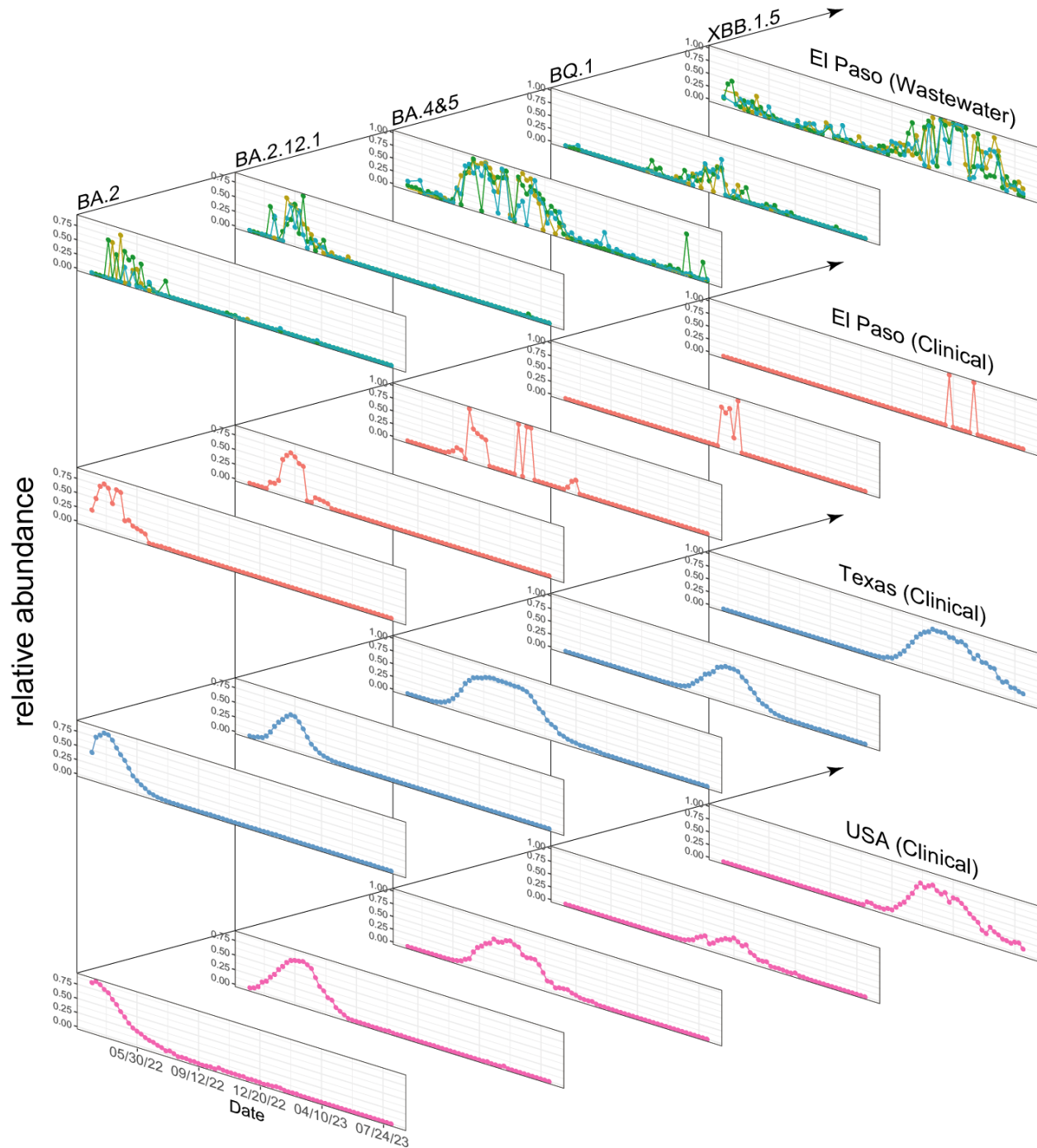


605 **Figure 1. RBD amplicon sequencing of wastewater reveals temporal dynamics of SARS-**  
606 **CoV-2 variants.** (A) Diagram of the RBD amplicon sequencing procedure. We specifically  
607 amplify the 337-504 aa sequence in the RBD region of SARS-CoV-2 spike gene. (B) Validation  
608 of the RBD amplicon sequencing protocol using the wild-type SARS-CoV-2 strain and BA.4&5.  
609 The bar plot shows the sequencing results of these samples, demonstrating that the resultant  
610 ratios closely match the original mixing ratios. (C) Viral load of SARS-CoV-2 per day per 100k  
611 people in the three sewersheds in the City of El Paso, TX from March 2022 to August 2023. (D-  
612 F) Relative abundance of SARS-CoV-2 variants revealed by RBD amplicon sequencing of  
613 wastewater samples from WWTPs A (D), B (E), and C (F) in the City of El Paso. (G) Relative  
614 abundance of SARS-CoV-2 variants from genomic sequencing of clinical samples in Texas.

615

616

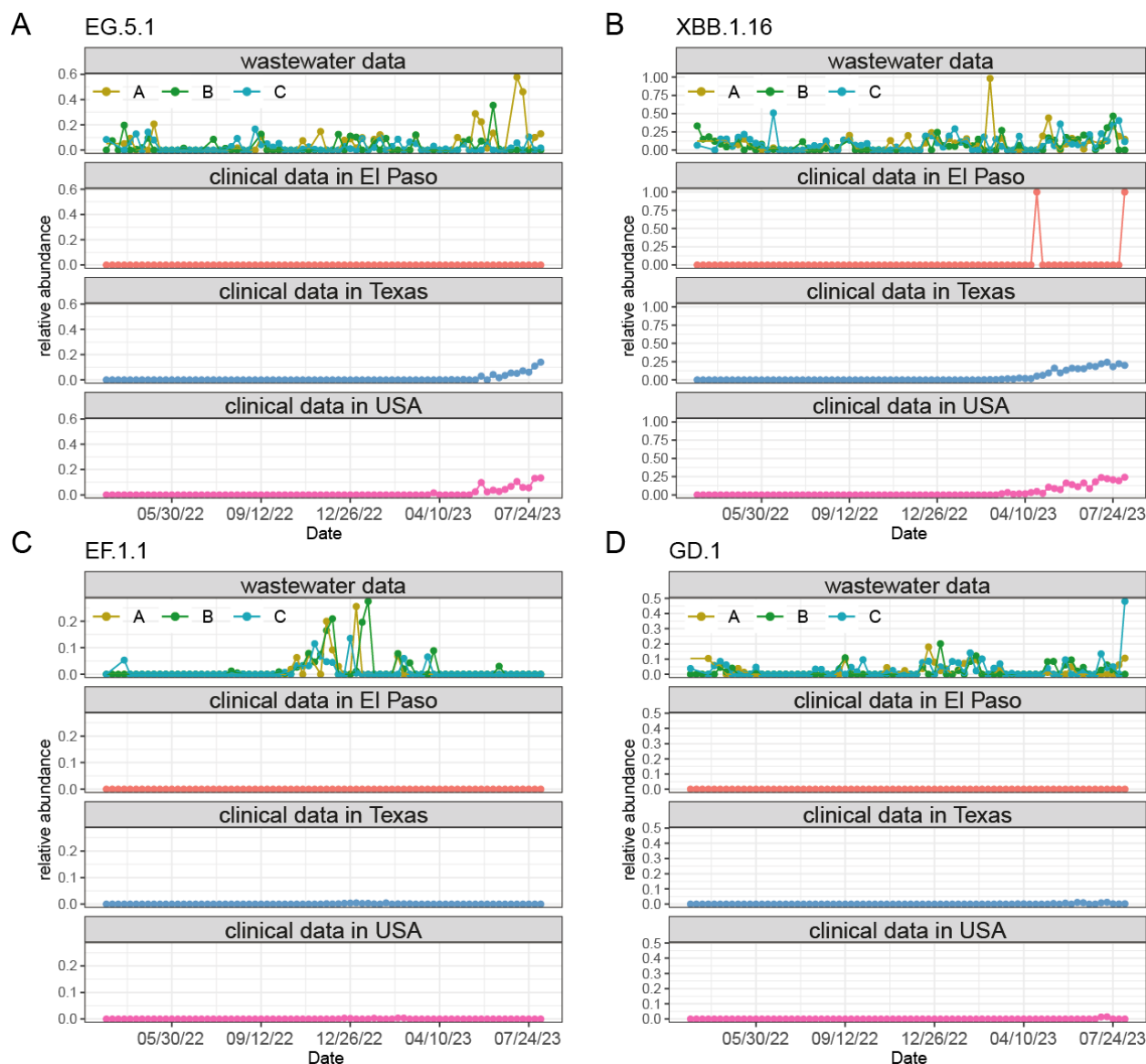
617



618

619 **Figure 2. Time-course of major SARS-CoV-2 variants identified from RBD amplicon**  
620 **sequencing of wastewater.** This figure presents the temporal dynamics of five major variants  
621 identified from three WWTPs alongside clinical data from El Paso, Texas, and the USA. Rows  
622 depict the progression of variant waves over time, while columns allow for a comparative  
623 analysis between the wastewater treatment plant data and clinical data, highlighting their  
624 similarities and trends.

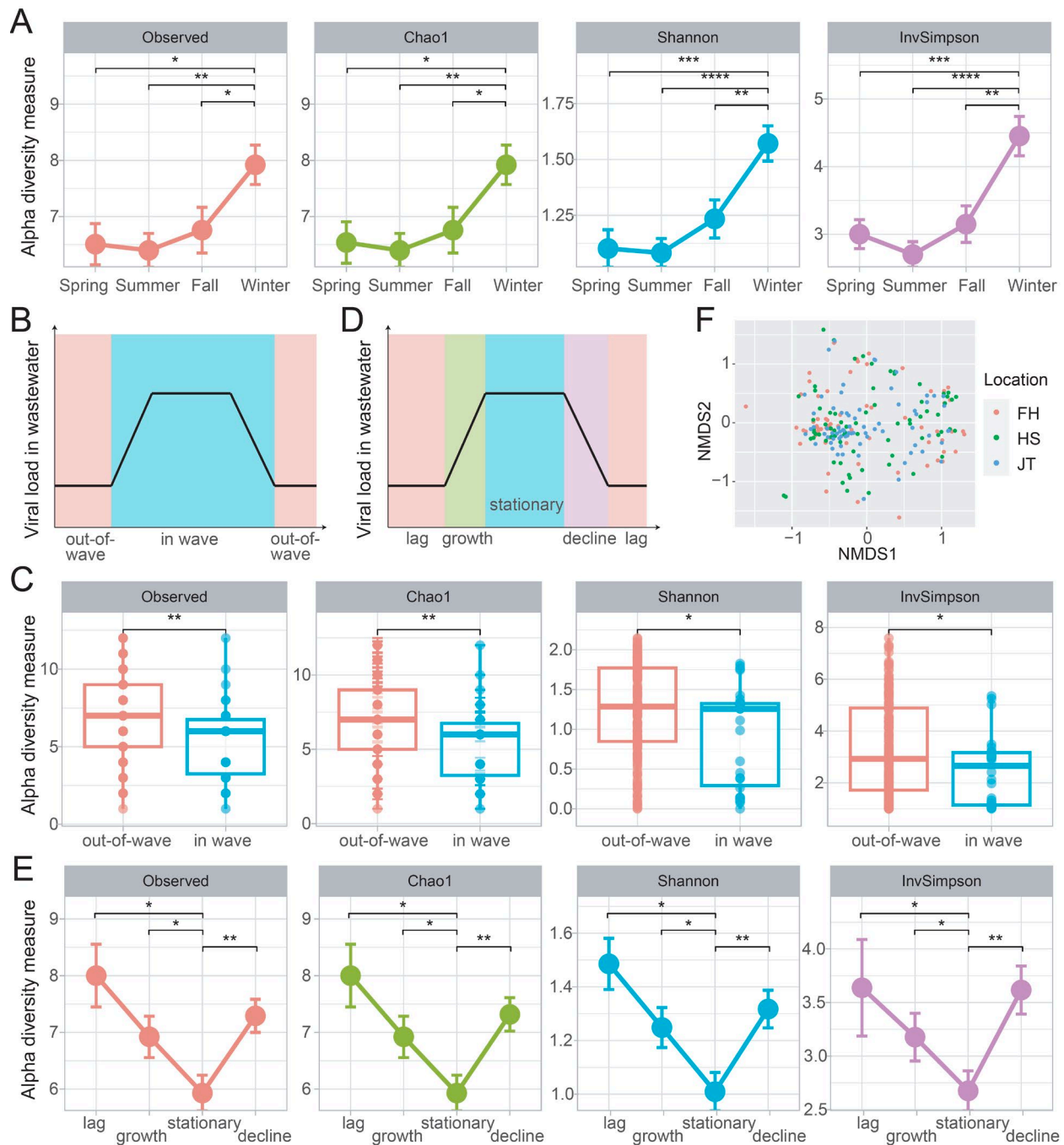
625



626

627 **Figure 4. Early detection and identification of unreported SARS-CoV-2 variants from RBD**  
628 **amplicon sequencing data. (A-B) The EG.5.1 and XBB.1.16 variants were detected circulating**  
629 **in the city earlier than their corresponding waves in clinical genome sequencing data from El**  
630 **Paso, Texas, and the USA. (C-D) The EF.1.1 and GD.1 variants were found in the city but were**  
631 **rarely reported in clinical genome sequencing data.**

632



633

634 **Figure 4. Epidemiological patterns of variant emergence and evolution.** (A) Alpha diversity

635 comparison across seasons in the three sewersheds. (B) Schematic diagram of the high

636 transmission (in-wave) and low transmission periods (out-of-wave) in an epidemic cycle. (C)

637 Comparison of alpha diversity between in-wave and out-of-wave samples. (D) Schematic

638 diagram of an epidemic cycle: lag, growth, stationary, and decline. (E) Alpha diversity

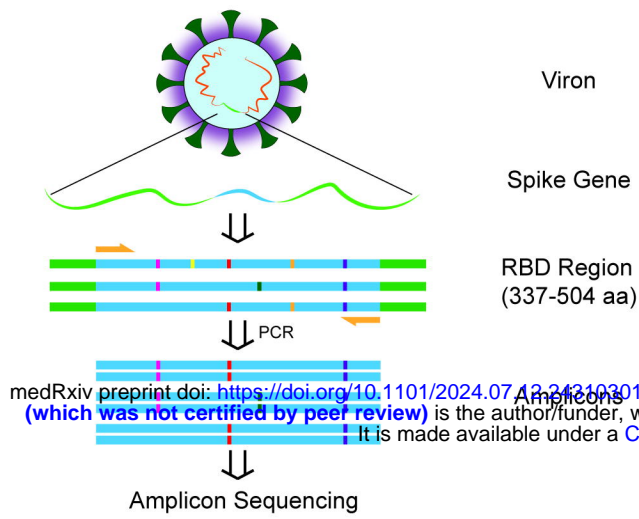
639 comparison across the four phases: lag, growth, stationary, and decline. (F) Beta diversity

640 analysis across all three WWTPs. No significant differences in viral diversity among the three  
641 sewersheds. Error bar: standard error; Wilcoxon rank-sum test was used for the group  
642 comparisons with significance: \*:  $p < 0.05$ ; \*\*:  $p < 0.01$ ; \*\*\* $p < 0.001$ . \*\*\*\*:  $p < 0.0001$ .

643

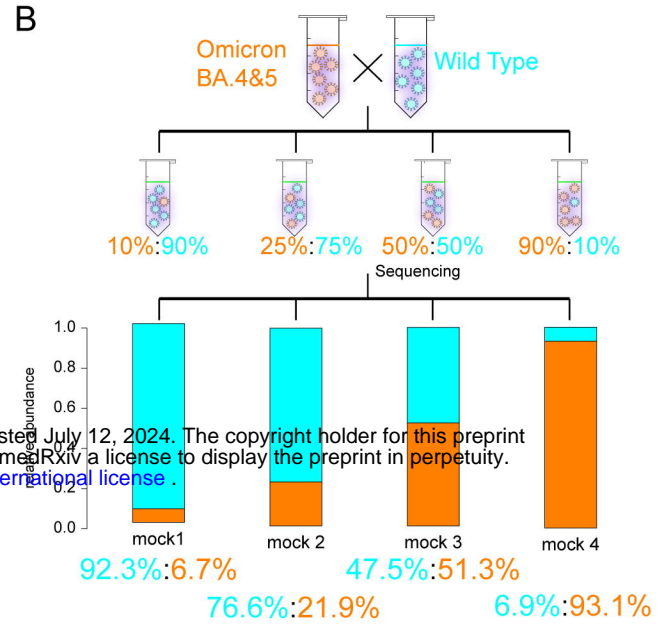
644

A

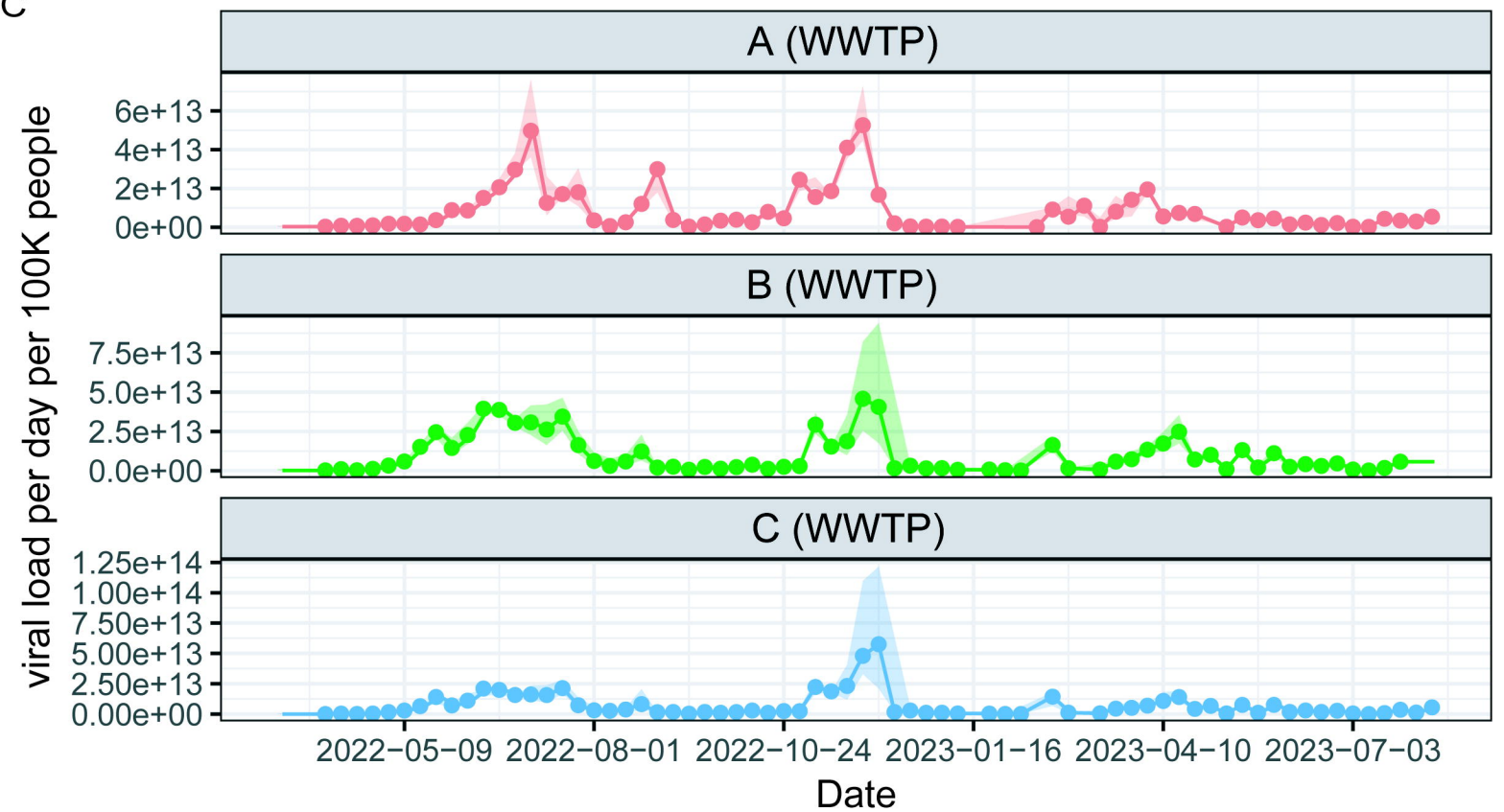


medRxiv preprint doi: <https://doi.org/10.1101/2024.07.12.2410301>; this version posted July 12, 2024. The copyright holder for this preprint (which was not certified by peer review) is the author/funder, who has granted medRxiv a license to display the preprint in perpetuity. It is made available under a [CC-BY-ND 4.0 International license](https://creativecommons.org/licenses/by-nd/4.0/).

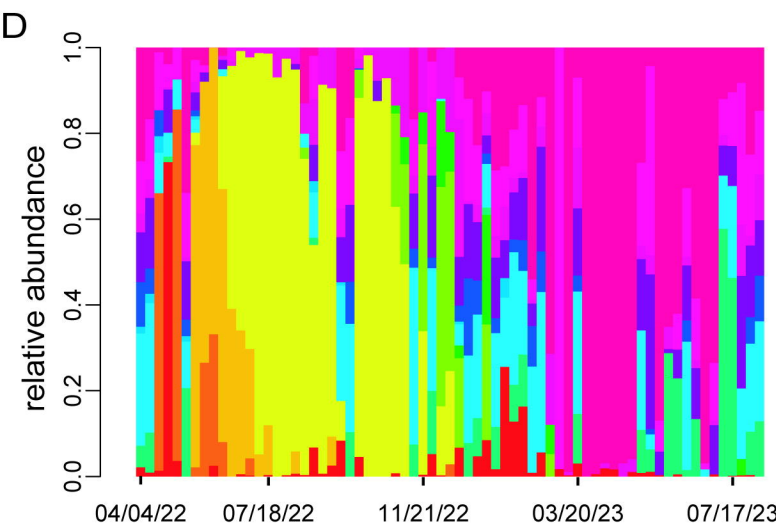
B



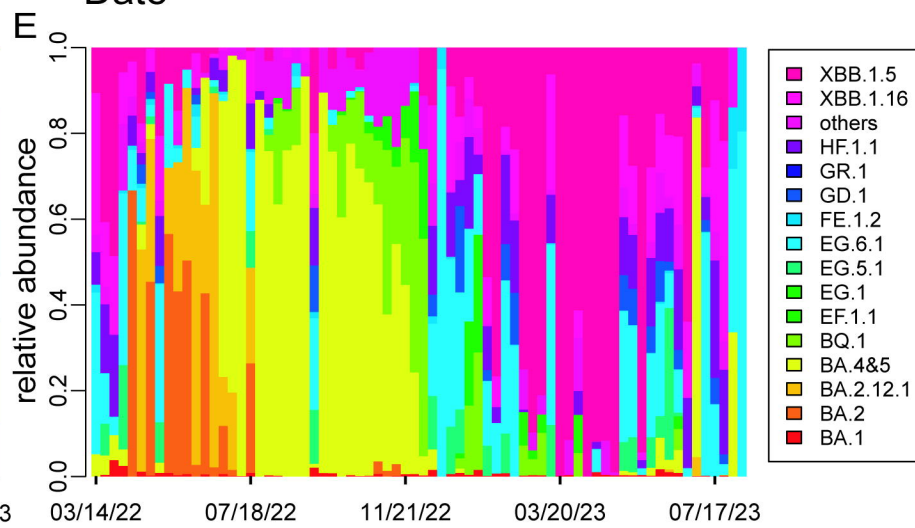
C



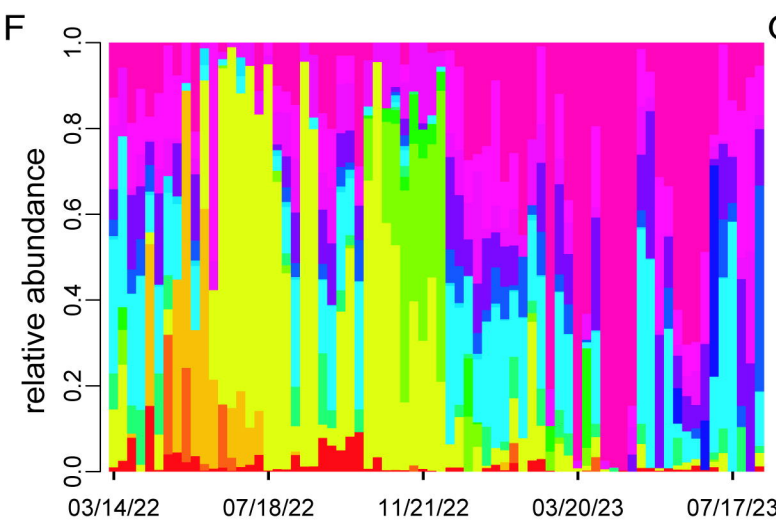
D



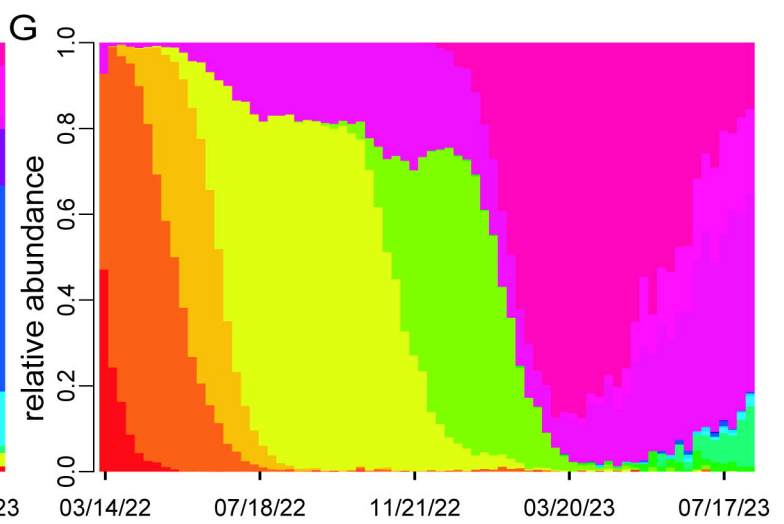
E



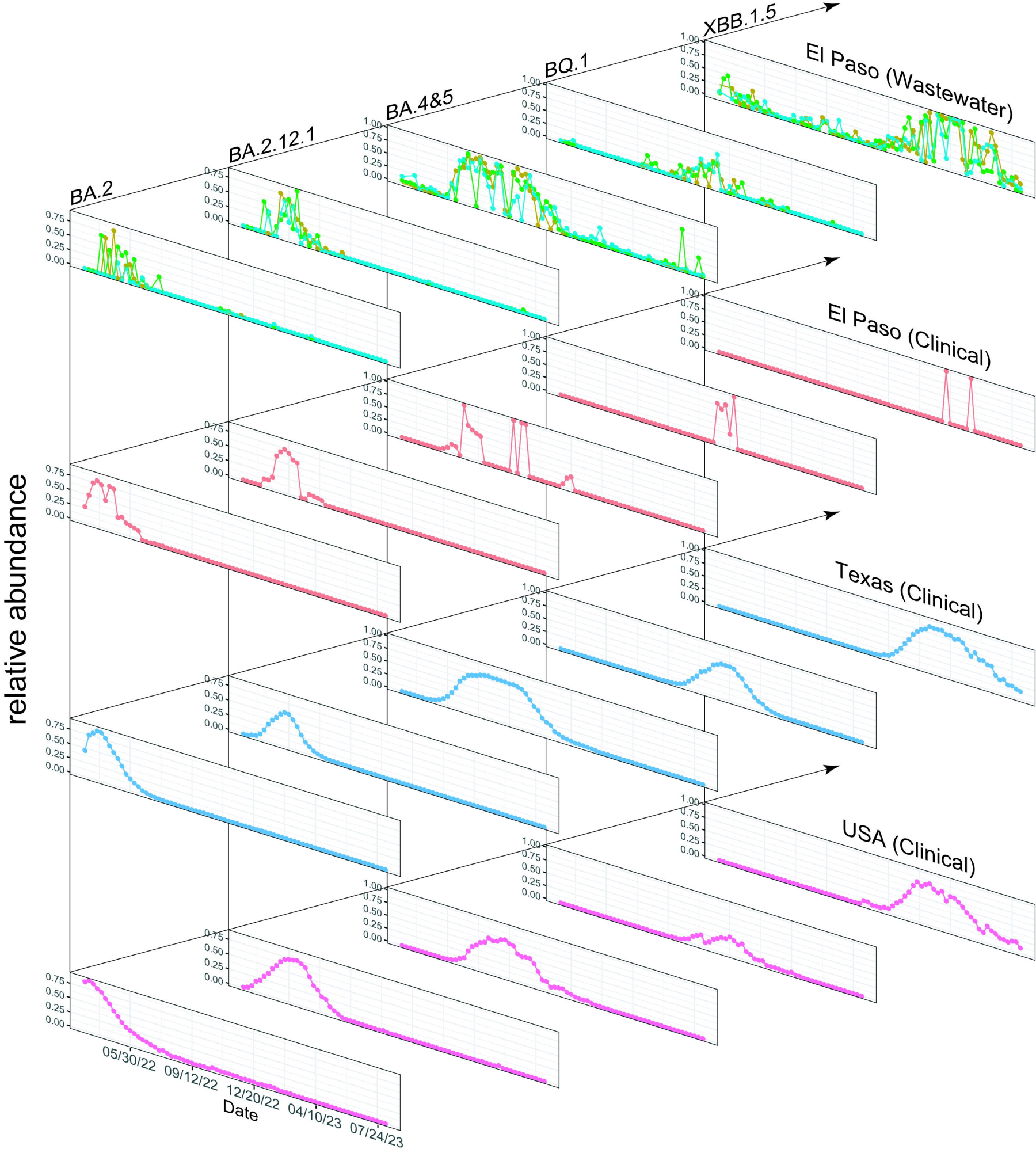
F



G

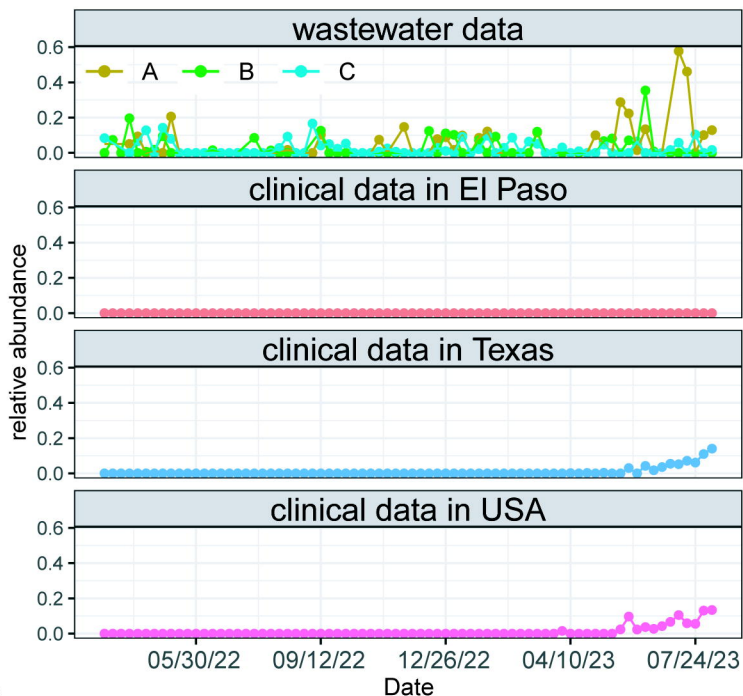






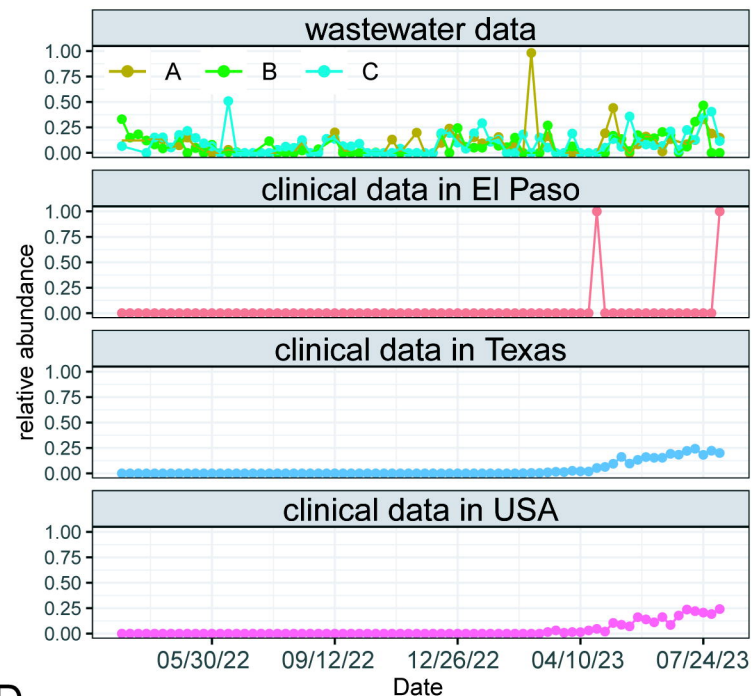
A

EG.5.1



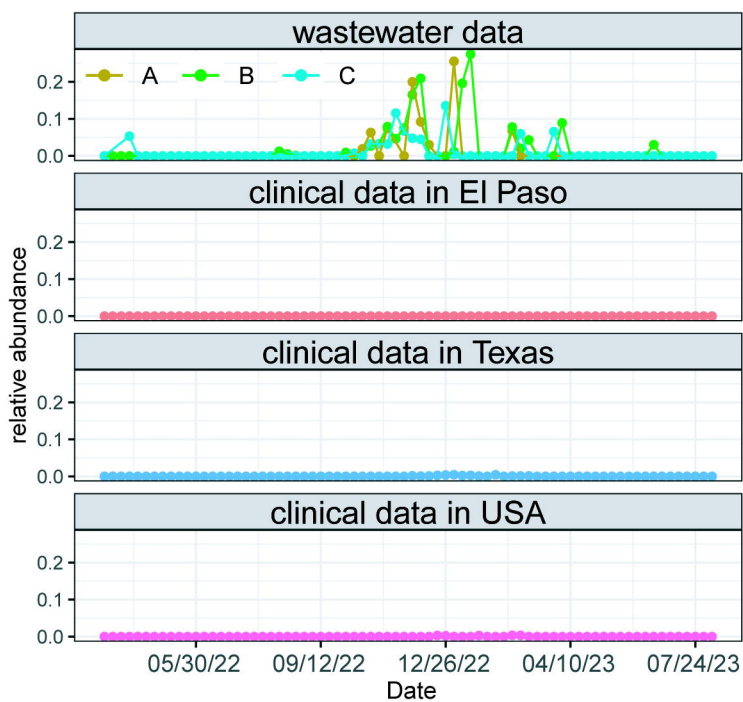
B

XBB.1.16



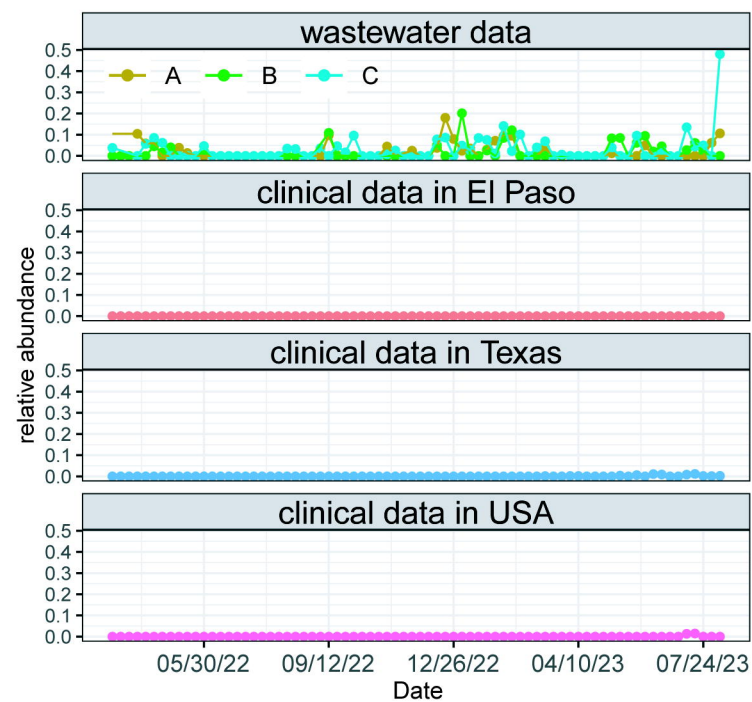
C

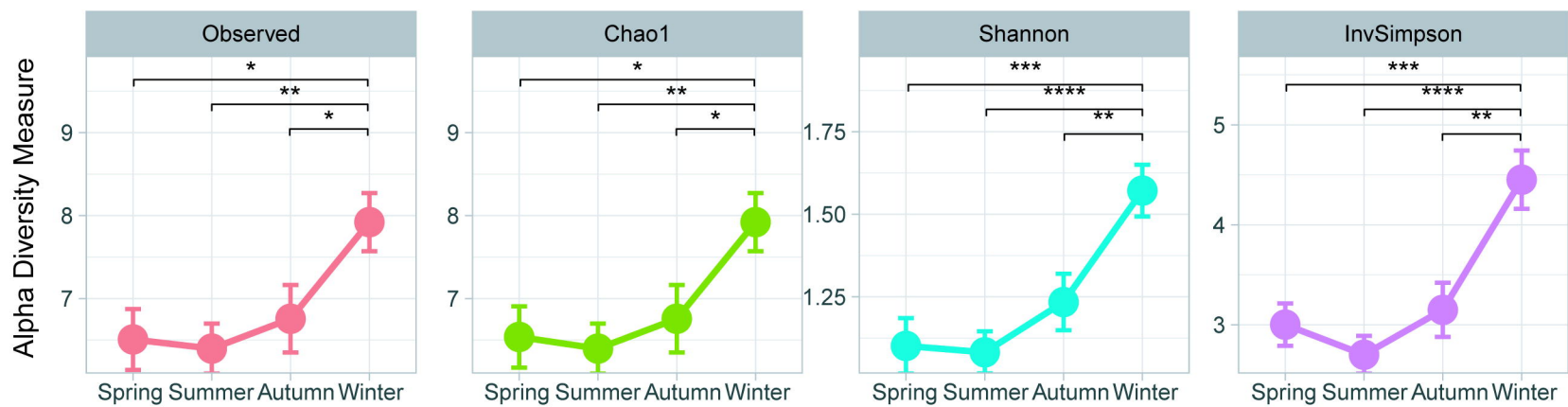
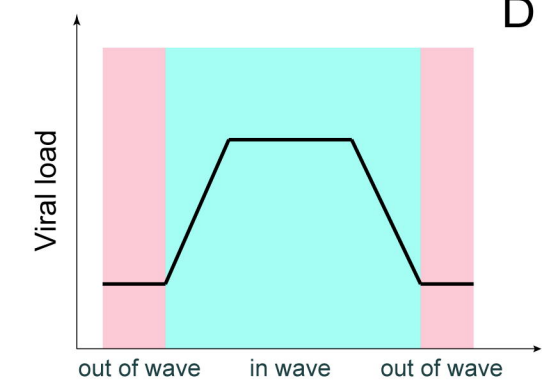
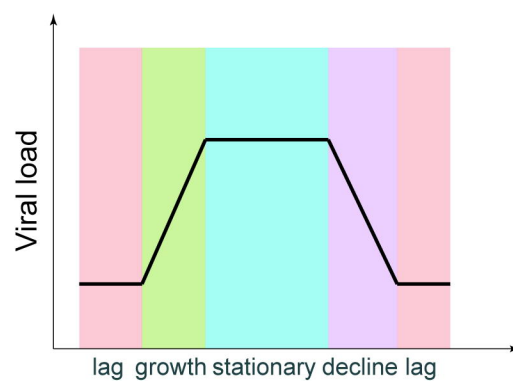
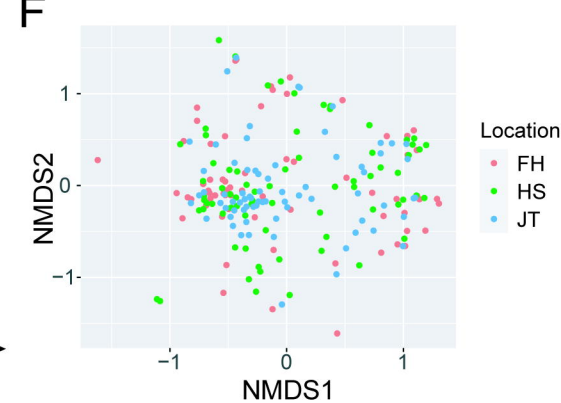
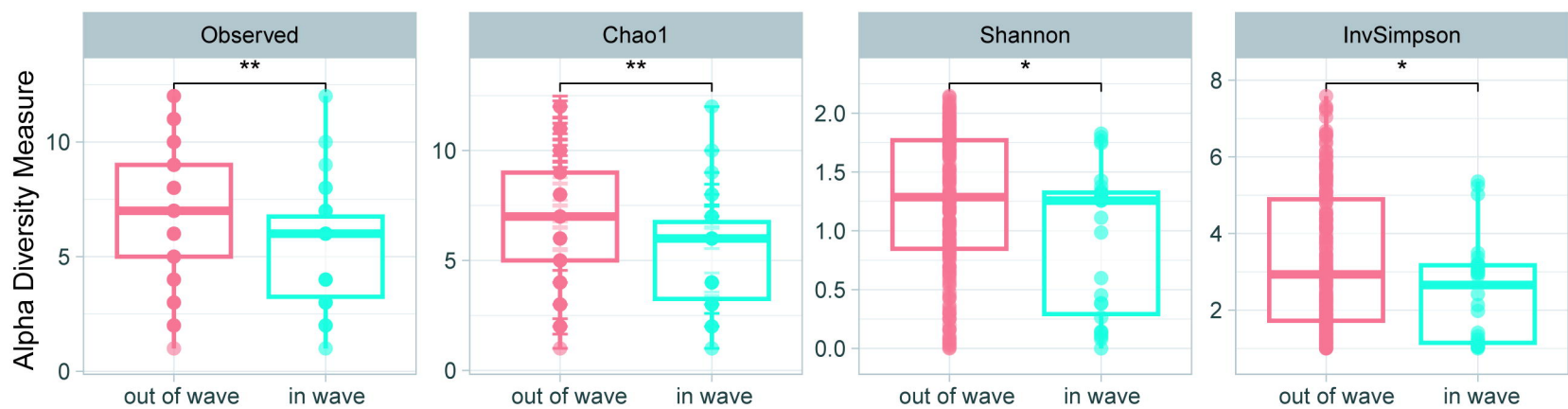
EF.1.1



D

GD.1



**A****B****D****F****C****E**